An Adaptative Ratio-Metric Analog-To-Digital Interface For Weakly-Coupled Resonant Sensors Based On Mutually Injection-Locked Oscillators

Ali Mostafa, Jérôme Juillard, João R. Raposo de O. Martins, Pietro Maris Ferreira

An Adaptative Ratio-Metric Analog-To-Digital Interface For Weakly-Coupled Resonant Sensors Based On Mutually Injection-Locked Oscillators

Ali Mostafa, Jérôme Juillard, João R. Raposo, Pietro M. Ferreira
GEEPS, UMR8507, CNRS, CentraleSupélec, UPSud, UPMC
Gif-sur-Yvette, France
{ali.mostafa, jerome.juillard joao-roberto.raposo}@centralesupelec.fr, maris@ieee.org

***Abstract*— In this paper, we propose a new ratio-metric interface for amplitude-modulated MEMS sensors based on mutually injection-locked oscillators (MILO). The two outputs are down-converted by a peak demodulator to improve the immunity to phase variation and noise. The peak values are then fed into a second-order discrete-time delta-sigma modulator that directly produces a digital ratio-metric output with a worst-case resolution greater than 16 bits and with input full scale of 0.6. The interface is clocked by the resonators output signal and is adapted for a sampling frequency up to 1MHz.**

Keywords—weakly-coupled resonators, amplitude demodulation, ratio-metric measurement, delta-sigma modulation

I. INTRODUCTION

Weakly-coupled resonant sensors (WCRs) based on amplitude ratio or phase difference measurements [1-2] have gained increasing attention over the past 10 years because of their significantly better long-term stability than conventional frequency-modulated (FM) resonant sensors, and their larger parametric sensitivity. Furthermore, amplitude-ratio modulated (RM) WCRs may have significant advantages over phase-modulated (PM) WCRs, in terms of resolution [3]. These distinctive advantages make RM WCRs well suited for high-end applications where high resolution (e.g. up to 16 bits) and long-term stability are required. However, RM or related output metrics such as [4]

$$\mathrm{TM} = \frac{X_1^{\varepsilon} - X_2^{\varepsilon}}{X_1^{\varepsilon} + X_2^{\varepsilon}} \tag{1}$$

where X_1^{ε} and X_2^{ε} are the amplitudes of the motional signals of the two weakly-coupled resonators, are not quasi-digital quantities, as opposed to phase or frequency. The most common approach to determine this quantity is to digitize the motional signals (at a sampling frequency much greater than the oscillation frequency) and perform a demodulation and a division in the digital domain [5]. However, this approach is not very amenable to integration, as it requires two high-resolution, high sampling frequency ADCs. Alternatively, one may perform demodulation in the analog domain. This approach requires either two high-resolution ADCs, or an analog voltage divider (VD) [6-7] and a single high-resolution ADC. Performing the demodulation in the analog domain considerably relaxes the constraints on the sampling frequency of the ADC(s).

The single ADC solution, which we investigate here, seems the most promising in terms of power consumption (in particular compared to two high sampling frequency ADCs), and robustness: in high-resolution applications, the two ADCs should be perfectly matched, which is not a trivial task, whether they operate at a large or a small sampling frequency.

The simplest way to implement a VD is the log-antilog network configuration [6], where the division is performed using three diode-connected transistors. However, the emitter saturation current varies significantly from one transistor to another and also with temperature. An alternative method is presented in [7], where the VD is implemented by a two-quadrant multiplier using only amplifiers and resistors. A relatively high resolution can be achieved at the cost of increasing complexity and power consumption. Alternatively, one may perform the division and the analog-to-digital conversion in a single step, as first described in [8]: the ratio of the demodulated amplitude signals is performed by using one signal as the input of a continuous-time delta-sigma (CT-ΔΣ) ADC, and the other signal as reference voltage. The great benefit of this solution is that one ADC is omitted. Furthermore, the inherent ratio-metric conversion scheme eliminates the need for an additional VD circuit, thus resulting in a compact circuit and a considerable reduction in power consumption. However, there are issues with this solution: CT-ΔΣ ADCs can only operate at a fixed clock frequency, f_s. The pole locations of the integrators do not scale with frequency as in discrete-time design (DT-ΔΣ). This limits the use of CT-ΔΣ in such applications where the master clock is generated by the resonators, and may vary from one sensor to another; CT-ΔΣ also have a limited common-mode rejection ratio (CMRR) because of mismatch in the input resistors or input transconductance, which may limit the common-mode input range [9].

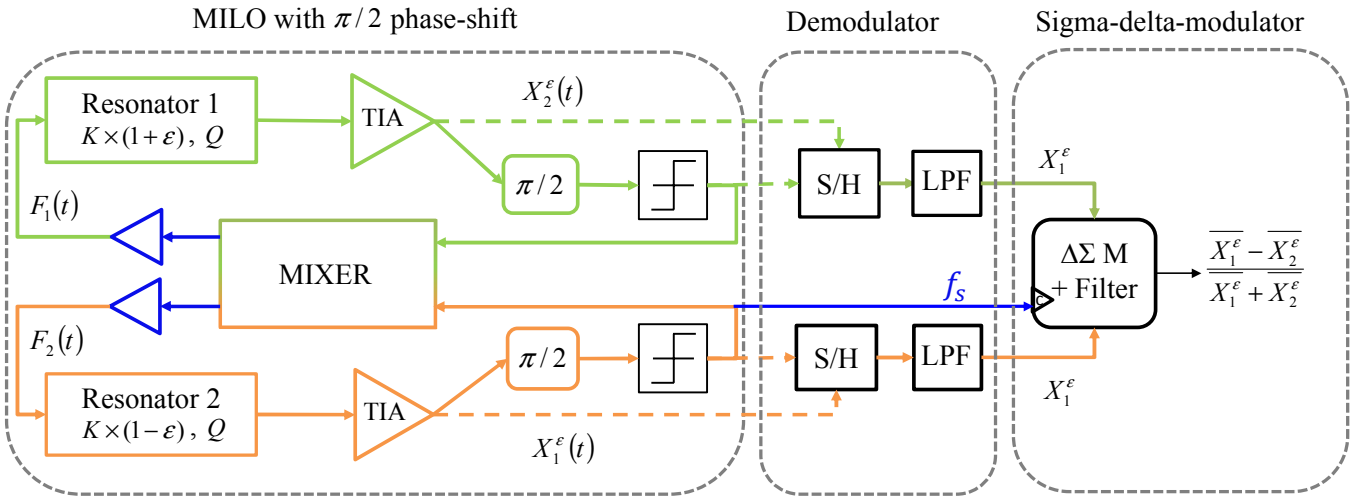

Fig. 1. High-level schematic of the MILO and the proposed ratio-metric interface

In this paper, a high-resolution ratio-metric interface for WCRs based on a mutually-injection locked oscillator (MILO) architecture is presented. Compared to the continuous time interface reported in [8], the proposed DT-ΔΣ architecture can operate for a wide frequency range with ultra-high resolution (greater than 16 bits). An appropriate demodulation technique for is also developed to enhance the signal to noise ratio (SNR). In section II the architecture selection for MILO and its interface is discussed. Simulation results are presented in section III. Finally, some concluding remarks and perspectives are given in Section IV.

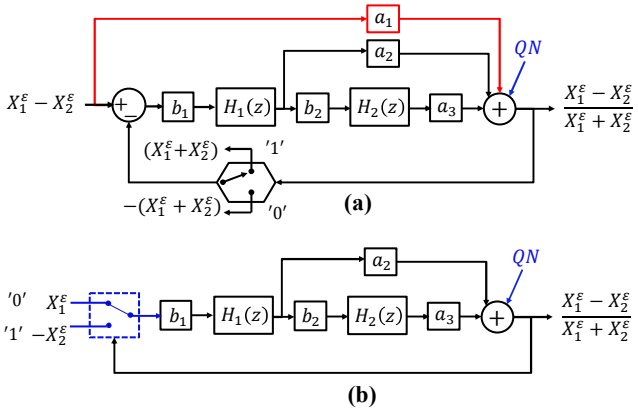

Fig. 2. Conventional full feed-forward architecture CIFF (a), modified implementation (b).

II. Proposed Architecture

The proposed architecture (Fig. 1) consists in a MILO, nominally oscillating at frequency f_s. The signals output by the transimpedance amplifiers (TIA) are amplitude-demodulated, filtered and used as inputs of a ratio-metric DT-ΔΣ modulator. The oscillating frequency, generated in the MILO, is used for clocking the amplitude demodulation blocks and the DT-ΔΣ modulator. Lowpass digital filtering then produces a high-resolution representation of the modified amplitude ratio. These blocks are detailed in the following sub-section.

A. MILO

MILOs consist in two resonators with nominally identical resonance frequencies and quality factors, coupled through a nonlinear mixer, as shown in Fig. 1. When a stiffness mismatch ε is induced between the resonators (e.g. electrostatically), the nonlinear mixer then ensures that the system remains in a phase-locked state, while providing high sensitivity to ε. Several MILO architectures may either be used as PM or TM sensors [4]. In the particular case when the loop phase shift is equal to $\pi/2$, the system shows a maximal TM sensitivity with a full scale of about 0.57 [11].

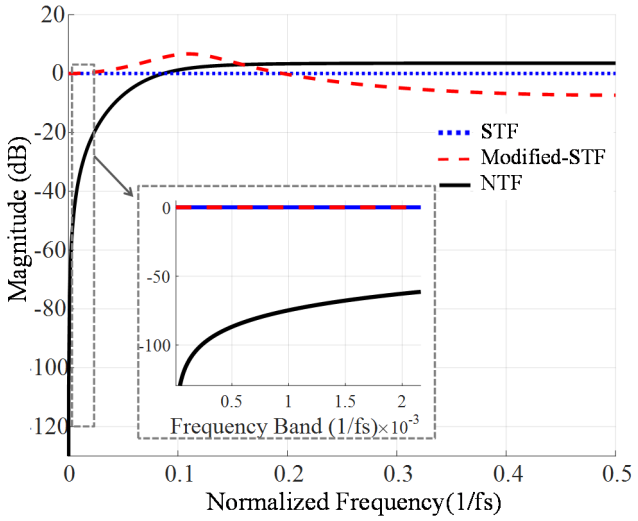

Fig. 3. Magnitude plot of second-order NTFs and STF of Fig. 2. $a_1 = a_2 = a_3 = 1$, $b_1 = 0.8$ $b_2 = 0.5$.

B. Demodulation technique

Using a synchronous demodulation technique may not be the best choice. In fact, as mentioned above, the two MILO's outputs are not in phase. Thus, a residual error may occur when dividing the demodulated signals, due to the leftover harmonics from the filtering operation. On the other hand, lowering the filter's cut-off frequency will limit the speed of the system. This last issue is a severe disadvantage when the

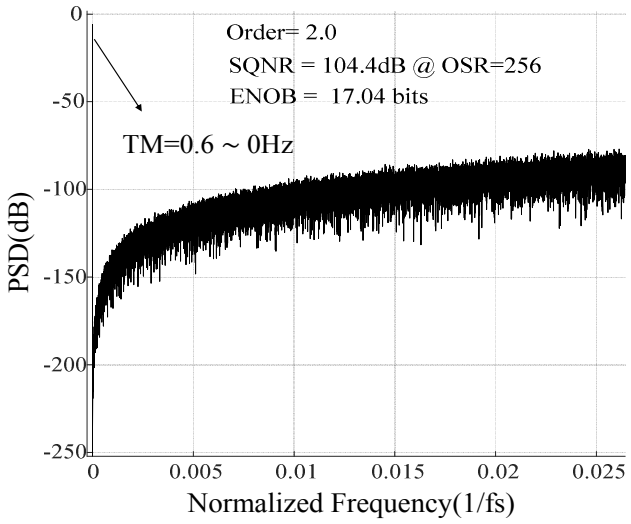

Fig. 4. PSD obtained from Simulink of the optimized ΔΣ with input signals of $X_1^\varepsilon = 0.8$ and $X_2^\varepsilon = 0.2$ ($X_1^\varepsilon - X_2^\varepsilon = 0.6$ $X_1^\varepsilon + X_2^\varepsilon = 1$). Hann-windowed FFT of 10^6 points.

settling time is critical. Taking samples around the voltage peaks may be an advantageous choice. Doing so leads to [10]: (i) a higher signal-to-noise ratio (SNR), (ii) an improved immunity to phase variation and (iii) relaxing the constraint related to the filter.

C. DT-ΔΣ architecture design

Due to their high-quality factor ($Q \geq 500$) and moderate resonance frequency ($f_s \leq 1\text{MHz}$), coupled resonator sensors are usually limited to narrow band applications, typically with a signal bandwidth $S_B = f_s / 2Q \leq 1\text{kHz}$. In practical, for a given resonators (f_s Q), the maximum resolution (nnominal Over Sampling Ratio (OSR_N)) is achieved when adapting the decimation filter bandwidth ($F_B = f_S / 2\text{OSR}_N$) to S_B. The OSR_N can be expressed as:

$$\text{OSR}_N = \frac{S_B}{F_B} \times Q \tag{2}$$

For instance, in worst case ($S_B^{wc} = 1\text{kHz}$, $Q^{wc} = 500$), the nominal is found to be $\approx 1.9\text{kHz}$ with an OSR_N^{wc} of 256. On the other hand, meeting the requirement of greater than 16 bits resolution with a 256 OSR_N^{wc} and a 1-bit quantizer, calls for a second or higher order modulator [9]. In this work, a discrete-time second-order single-bit full feed-forward architecture (CIFF) was chosen as a basis (Fig. 2-a). The corresponding noise transfer function NTF(z) and signal transfer function STF(z) can be expressed as:

$$\text{STF}(z) = \frac{(z-1)^2 a_1 + (z-1) a_2 b_1 + a_3 b_1 b_2}{(z-1)^2 + (z-1) a_2 b_1 + a_3 b_1 b_2} \tag{3}$$

$$\text{NTF}(z) = \frac{(z-1)^2}{(z-1)^2 + (z-1) a_2 b_1 + a_3 b_1 b_2} \tag{4}$$

As expected from (3) and shown in Fig. 3, in low frequency, the input to quantizer feedforward path has almost no impact on the STF. In addition, the NTF does not depend on a_1. Thus, this branch can be omitted, leading to a simpler and more compact architecture (Fig. 2-b). The other coefficients a_2, a_3, b_1 and b_2 are optimized, using ΔΣ toolbox [9], to find a worst-case resolution of (>16 bits) for an input full scale slightly larger than 0.57. The optimized NTF which satisfy these requirements is found to be:

$$\text{NTF}(z) = \frac{(z-1)^2}{z^2 - 1.2z + 06} \tag{5}$$

The corresponding output power spectral density (PSD) is depicted in Fig. 4.

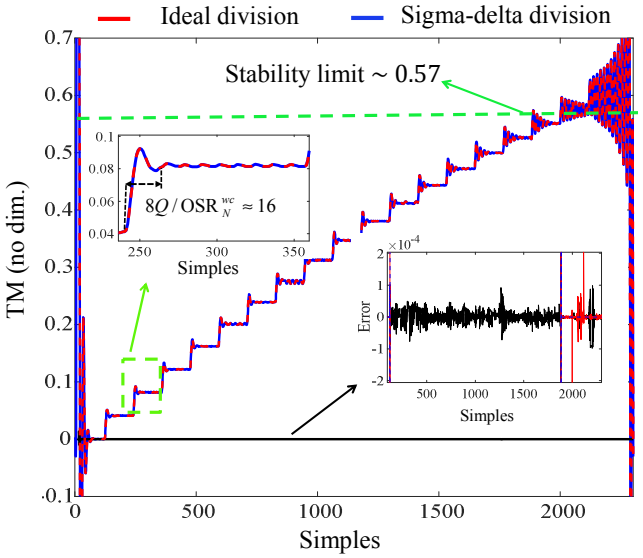

Fig. 5. Transient simulation of the system of Fig. 1.

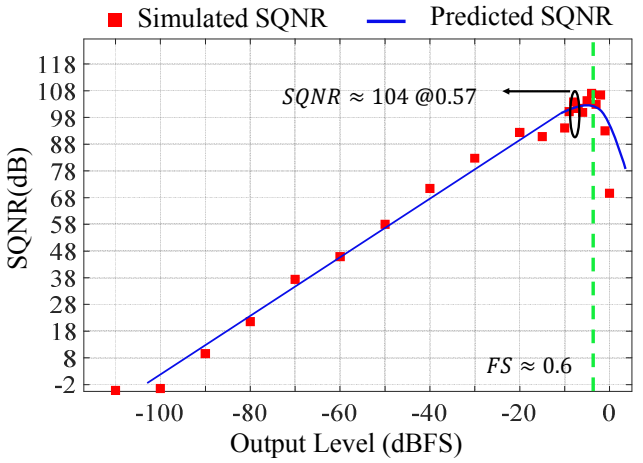

Fig. 6. SQNR as a function of the output level.

III. Simulation Results

In Fig. 5 the architecture of Fig. 1 is simulated with Simulink in the worst case, for two identical ($Q^{wc} = 500$, $f_s = 1\text{MHz}$), linear resonators, along the system locking range. The input ε is applied differentially to the two resonators and stepped every 3.10^3 samples (approximately

$8Q$ samples, or 7.5 times the resonators' 98% settling time). The output value of TM is then averaged with the decimation filter with OSR of 256 to 117 samples/s. The ideal and the ΔΣ responses are perfectly matched. The residual error is limited to the 'quantization white noise': it is plotted in Fig. 6 as a function of output level. At the full-scale value, the system shows a SQNR of 104.4dB (17bits). Fig. 6 also points out that the locking range of the system is not limited by the dynamic range of the modulator, since there is no distortion for an output of 0.57.

IV. Conclusion

An adaptative ratio metric interface for WCRSs based MILO has been presented. Simulation of the ideal model shows its high accuracy for a ratio-metric measurement, theoretically with a worst-case resolution of 17 bits. In addition, since our solution is based on a second-order modulator, this resolution can be increased by approximately 2.2 bits if the OSR or Q is doubled (2) [9]. Thus, in most cases, the ultimate resolution will be limited by the electronic noise. Further studies should address the issue of flicker noise, since the input signals are in a low frequency band. Our continuing work will then focus on the effect of the component non-idealities of the modulator, including noise, Op-amp finite gain and linearity.

References

[1] J. Juillard, P. Prache, and N. Barniol, "Analysis of mutually injection-locked oscillators for differential resonant sensing," IEEE Trans. Circuits Syst. I Regul. Pap., vol. 63, no. 7, pp. 1055–1066, 2016.

[2] C. Zhao, M. H. Montaseri, G. S. Wood, S. H. Pu, A. A. Seshia, and M. Kraft, "A review on coupled MEMS resonators for sensing applications utilizing mode localization," Sensors Actuators, A Phys., vol. 249, pp. 93–111, 2016.

[3] J. Juillard, A. Mostafa, P. M. Ferreira, "Analysis of resonant sensors based on mutually injection locked oscillators beyond the critical Duffing amplitude", European Frequency and Time Forum, 2018 pp. 114-118, 2018.K.

[4] M. R. Nabavi, M. A. P. Pertijs, and S. Nihtianov, "An interface for eddy-current displacement sensors with 15-bit resolution and 20 mhz excitation," IEEE J. Solid-State Circuits, vol. 48, no. 11, pp. 2868–2881, 2013

[5] M. Pandit, S. Member, C. Zhao, G. Sobreviela, A. Mustafazade, and S. Du, "Closed-loop Characterization of Noise and Stability in a Mode-localized Resonant MEMS Sensor," IEEE Trans. Ultrason. Ferroelectr. Freq. Control, 2018, preprint.

[6] J. G. Graeme, "Applications of Op Amps: third generation techniques,"1973.

[7] K. C. Selvam and S. Latha, "A Novel Voltage Divider Circuit," ETASR - Eng. Technol. Appl. Sci. Res., vol. 2, no. 5, pp. 278–280, 2012.

[8] A. Fekri, M. Nabavi, N. Radelji, Z. Chang, M. Pertijs, and S. Nihtianov, "An Eddy-Current Displacement-to-Digital Converter Based on a Ratio-Metric Delta-Sigma ADC," pp. 403–406, 2014.

[9] R. Schreier, G. C. Temes, "Understanding Delta-Sigma Data Converters,"2005.

[10] M. R. Nabavi and S. Nihtianov, "A novel interface for eddy current displacement sensors," IEEE Trans. Instrum. Meas., vol. 58, no. 5, pp. 1623–1632, 2009.

[11] J. Juillard, A. Mostafa, P. M. Ferreira, "Nonlinear enhancement of locking range of mutually injection-locked oscillators for resonant sensing applications", European Frequency and Time Forum, 2018, pp. 109-113, 2018.